ภาคผนวก
บทความที่ส่งตีพิมพ์

Chiang Mai J. Sci. 2008; 35(3) : 437-446
www.science.cmu.ac.th/journal-science/josci.html
Contributed Paper

Adaptive Control for a One-Link Robot Arm Actuated by Pneumatic Muscles

Tarapong Karnjanaparichat and Radom Pongvuthithum*
Department of Mechanical Engineering, Chiang Mai University, Chiang Mai 50200, Thailand.
*Author for correspondence; e-mail: radomp@gmail.com

Received: 1 August 2008
Accepted: 31 August 2008.

ABSTRACT

Presently artificial pneumatic muscles are used in various applications due to their simple construction, lightweight and high force to weight ratio. However, controls of various mechanical systems actuated by pneumatic muscles are facing various problems. The parameters of the muscles are nonlinear and time-varying due to temperature change and the deterioration of the pneumatic muscle materials when the muscles are used for an extended period of time. Therefore, adaptive control is suitable to solve control problems for the pneumatic muscles since it can be designed to be independent of all system parameters and be able to adapt to certain changes of the system parameters.

In this paper, we study the problem of adaptive output tracking for a one-link robot arm actuated by two opposing pneumatic muscle groups. The two muscle groups are arranged to simulate the physiological model of the bicep-tricep system.

An adaptive controller is designed under the condition that all physical parameters, such as the pneumatic muscle coefficients, length of the arm, mass, moment of inertia and etc., are unknown. Under this condition, we can prove that closed-loop trajectory of the joint angle can follow any C^1 signal and the angle error will be within a prescribed error in a finite time. Simulations are presented to demonstrate the robustness of our adaptive controller under serve changes of the system parameters.

Keywords: output tracking, pneumatic muscles, adaptive control.

1. INTRODUCTION

The artificial pneumatic muscles are used in various applications such as robotics, bio-robotics, biomechanics, artificial limb replacements and many industry tasks. The advantages of the pneumatic muscles are the ease of use compared to standard pneumatic cylinders and their simple construction. The pneumatic muscles are also soft, lightweight and have a high power/force to weight ratio. In addition, the pneumatic muscles can be twisted axially i.e. not aligned and bended. These features make pneumatic muscles a major interest for the researchers and hobbyists.

The mathematical models of pneumatic muscle have been developed in two different ways, dynamics and static models. Chou and Hannaford, [1, 2], and Tondu and Lopez [3] developed static models by using virtual work to find the relation of force, pressure

and lengths of muscle. On the other hand, the dynamics model, developed by Reynolds et al. [4, 5] models the muscles by connecting a spring, a damping and a contractile element in parallel. However, this paper only focus on the dynamics model since it has been widely used in various control applications [6-10] and also offers a simpler structure of the muscle comparing to the static model.

The control of pneumatic muscles is difficult due to the physical parameters being nonlinear and time-varying. Many researchers have proposed control schemes for solving control problems of uncertain mechanical systems actuated by pneumatic muscles. For example, Lilly [6] proposed a sliding-mode adaptive controller for a planar robot arm actuated by pneumatic muscles. This adaptive controller requires the exact forms of the nonlinear functions and the system mechanical properties, e.g. the link masses, lengths and inertias. In [7], Lilly and Quesada extended the result in [6] to a two-link arm. Lilly and Yang [8] developed a robust controller based on sliding-mode for a planar robot arm with a load at the end point. The robust controllers in [6-8] require the information on the bounds of system parameters. In addition, in the case of sliding mode controller, chattering can occur due to the controller being a discontinuous function. Taking another approach, Lilly and Chang, [9, 10], developed Fuzzy predictive controller for a two-link arm actuated pneumatic muscles. A fuzzy model was developed based on linearized model around operating point on state space, therefore all of system parameters must be known precisely.

For pneumatic muscles, muscle property changes due to temperature changes and the deterioration of the pneumatic muscle materials when the muscles are in use for an extended period of time are common. Therefore, the existing controllers are not suitable in practice. To solve the problem, we should develop a continuous controller that is independent of all system parameters and can adapt the system parameter changes. In this paper, we will focus on designing an adaptive controller for a one-link robot arm actuated by pneumatic muscles. The proposed control scheme is based on a monotone adaptive control studied in [11, 12]. The controller is obtained under the condition that all of physical parameters of the robot arm and the muscles are unknown. Under this condition, it can be proved that the robot arm can follow any C^1 signal and the angle error will be within a prescribed error in a finite time.

The remaining of the paper is organized as follows. Section 2 contains concepts of pneumatic muscle model and the dynamics of one-link arm actuated by pneumatic muscles. Design methodology of the monotone adaptive controller is presented in Section 3. Simulation results demonstrating our controller performance are in Section 4. Finally, conclusions are drawn in Section 5.

2. DYNAMICS OF A ONE-LINK ROBOT ARM ACTUATED BY PNEUMATIC MUSCLES

2.1 Dynamics Model of Pneumatic Muscles

In [4, 5] a pneumatic muscle is modeled by three elements, a spring a damping and a contractile, connecting in parallel, see Figure 1. The total force exerted by the muscle on the mass is

$$R = F(P) - B(P)\dot{y} - K(P)y \qquad (1)$$

where F is the force exerted by the contractile element, B is the damping coefficient and K is the spring coefficient. Using data from experiments, the coefficients

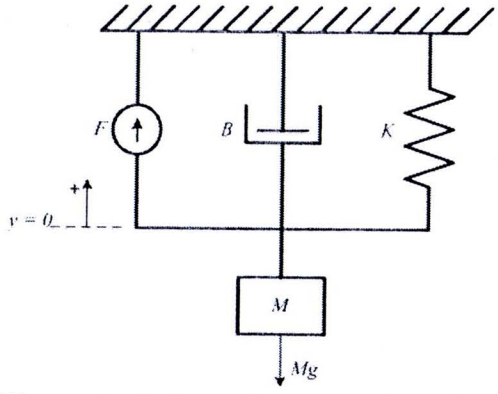

Figure 1. A three-element model of the pneumatic muscle.

were formulated as polynomial functions of the input pressure of the muscle.

To find the coefficient functions of the three-elements, the muscle was hung vertically with a mass attached at the lower end. Then, the muscle was inflated and held at various constant P. Let $y = 0$ be the position of the mass when the muscle is completely deflated see Figure 2. The position y and the values of the three coefficients were determined by perturbing the load at each constant P. Under the assumption that the spring and damping coefficient functions determined by perturbation of the load at constant P are the same functions as obtained in the dynamic condition, the coefficient functions were formulated by the least square method.

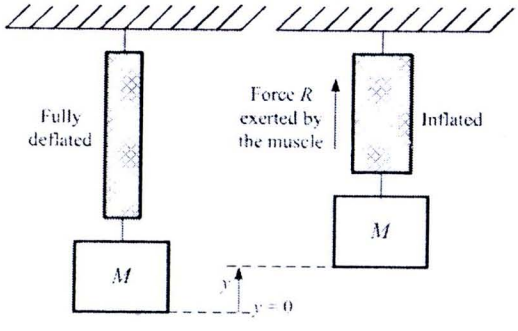

Figure 2. The pneumatic muscle is actuating a mass.

According to [4], their muscle coefficient functions of the three elements are given as:

$$K(P) = K_0 + K_1 P$$
$$= 32.58 + 1.209P \quad (2)$$
$$B(P) = B_{0i} + B_{1i} P$$
$$= 5.748 + 0.2719P \text{ (Inflation)} \quad (3a)$$
$$B(P) = B_{0d} - B_{1d} P$$
$$= 3.41 - 0.0316P \text{ (Deflation)} \quad (3b)$$
$$F(P) = F_1 P - F_2 P^2$$
$$= 3.77P - 0.0138P^2 \quad (4)$$

The coefficients in (2)-(4) are applicable for pressure in the range of $0 \le P \le 130$ psi.

2.2 Dynamics of a One-link Rigid Arm

Consider a rigid link shown in Figure 3. Let q denote the angle of the joint, l denotes the length of the link, l_c denotes the distance from origin point to the center of mass.

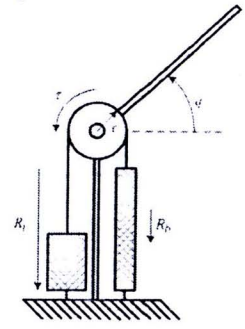

Figure 3. The one-link rigid arm.

The kinetic energy of the system is

$$T = \frac{1}{2} m v_c^2 + \frac{1}{2} I \omega^2$$
$$= \frac{1}{2} m l_c^2 \dot{q}^2 + \frac{1}{2} I \dot{q}^2 \quad (5)$$

where I the moment of inertia of the link and the potential energy is

$$V = m g l_c \sin q \quad (6)$$

The Lagrange function is

$$L = T - V$$
$$= \frac{1}{2} m l_c^2 \dot{q}^2 + \frac{1}{2} I \dot{q}^2 - m g l_c \sin q \quad (7)$$

According to Lagrange's equation, $\frac{d}{dt}\frac{\partial L}{\partial \dot{q}} - \frac{\partial L}{\partial q} = \tau$. The dynamics equation of the one rigid link is

$$ml^2\ddot{q} + I\ddot{q} + mgl_c \cos q = \tau \quad (8)$$

where τ is the torque for driving the arm joint.

2.3 Dynamics of the Pneumatic Muscle Actuator in a Robot Arm

Consider a pneumatic muscle pair putting into antagonism similar to actuators in the physiological model of the bicep-tricep system in Figure 4. The muscle pairs are connected by means of a chain driving a sprocket. The group of bicep muscles is not necessary to have the same muscle coefficients as the group of tricep muscles. The force difference between the agonist and the antagonist generates a positive or negative torque.

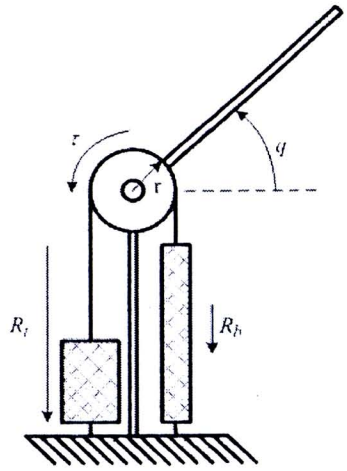

Figure 4. The pneumatic muscle pairs tied together around a sprocket.

Assume that the n pneumatic muscle pairs tied together around a sprocket of radius r as in Figure 4, with the connecting line rigidly attached to the sprocket to prevent slipping. The torque produced to the sprocket by the muscle pairs is

$$\tau = \tau_t - \tau_b = (R_t - R_b)r \quad (9)$$

where R_b and R_t are the total force exerted by an individual group of bicep and tricep muscles respectively. When the force $R_t > R_b$, then the torque exerted on the joint is counterclockwise and vice versa. From (1), we have

$$R_b = n(F_b - K_b x_b - B_b \dot{x}_b) \quad (10a)$$

$$R_t = n(F_t - K_t x_t - B_t \dot{x}_t) \quad (10b)$$

where x_b is the length of bicep muscles and x_t is the length of tricep muscles. Substitute (10) into (9), then the total torque delivered to the sprocket is given by

$$\tau = n(F_t - K_t x_t - B_t \dot{x}_t - F_b + K_b x_b + B_b \dot{x}_b)r \quad (11)$$

where F_b, K_b and B_b depend on the input pressure of bicep muscles and F_t, K_t and B_t depend on the input pressure of tricep muscles.

A joint angle of $q = -90°$ corresponds to the tricep muscles being fully extended and the bicep fully contracted, and $q = 90°$ corresponds to the tricep muscles being fully contracted and the bicep fully extended. Therefore, the muscle lengths x_t and x_b can be expressed in terms of q as

$$x_b = \left(\frac{\pi}{2} - q\right)r \quad (12a)$$

$$x_t = \left(q + \frac{\pi}{2}\right)r \quad (12b)$$

Let the internal pressure of the bicep muscles P_b and the tricep muscles P_t be

$$P_b = P_{0b} - \Delta p \quad (13a)$$

$$P_t = P_{0t} + \Delta p \quad (13b)$$

where P_{0b} and P_{0t} are arbitrary positive nominal constant pressures and Δp is the control input. With the definition (13), the antagonist pairs become a single-input system with input Δp.

From (11)-(13) and the coefficient functions (2)-(4), the torque can be written as

$$\tau = a_A \Delta p^2 - (b_B(t)\dot{q} + a_C q + a_D)\Delta p + b_E(t)\dot{q} + a_F q + a_G \quad (14)$$

where

$$a_A = n(F_{2b} - F_{2t})r \quad (15a)$$

$$b_B(t)=\begin{cases}-n(B_{1bi}+B_{1td})r^2, & \dot{q}<0\\ 0, & \dot{q}=0\\ n(B_{1ti}+B_{1bd})r^2, & \dot{q}>0\end{cases} \quad (15b)$$

$$a_C = n(K_{1t}-K_{1b})r^2 \quad (15c)$$

$$a_D=\frac{n}{2}(4F_{2t}P_{0t}+4F_{2b}P_{0b}+rK_{1b}\pi - 2F_{1t}-2F_{1b})r \quad (15d)$$

$$b_E(t)=\begin{cases}-n(B_{bti}-B_{tdi}P_{0t}+B_{bdi}+B_{bti}P_{0b})r^2, & \dot{q}<0\\ 0, & \dot{q}=0\\ -n(B_{bdi}+B_{tti}P_{0t}+B_{bti}-B_{bti}P_{0b})r^2, & \dot{q}>0\end{cases} \quad (15e)$$

$$a_F=-n(K_{1t}P_{0b}+K_{1t}P_{0t}+K_{0b}+K_{0t})r^2 \quad (15f)$$

$$a_G=-\frac{n}{2}(-rK_{1t}P_{0t}\pi+2F_{1t}P_{0t}-rK_{0t}\pi + 2F_{2t}P_{0t}^2-2F_{2b}P_{0b}^2-2F_{1t}P_{0b}^2 + rK_{0t}\pi+rK_{1t}P_{0t}\pi)r \quad (15g)$$

In (15), b and t subscripts indicate the coefficients of bicep and tricep muscles respectively. The subscripts, i and d, on the coefficient B denote whether the muscles are being inflated and deflated respectively.

Combining the dynamics of the one rigid link arm from (8) and the dynamic of the pneumatic muscle, (14)-(15), we can arrive at the following model for the one-link planar robot arm actuated by pneumatic muscles in Figure 4.

$$\ddot{q}=\bar{a}_A\Delta p^2-f\left(q,\dot{q},b_B(t)\right)\Delta p+h\left(q,\dot{q},b_E(t)\right) \quad (16)$$

where

$$\bar{a}_A=\frac{a_A}{ml_c^2+I} \quad (17a)$$

$$f\left(q,\dot{q},b_B(t)\right)=\frac{b_B(t)\dot{q}+a_C q+a_D}{ml_c^2+I} \quad (17b)$$

$$h\left(q,\dot{q},b_E(t)\right)=\frac{b_E(t)\dot{q}+a_E q+a_G}{ml_c^2+I}-\frac{mg\cos q}{ml_c^2+I} \quad (17c)$$

3. Adaptive Control for a One-Link Robot Arm Actuated by Pneumatic Muscles

3.1 Problem Statement

Let $x_1=q$ and $x_2=\dot{q}$ Then, the system of one-link robot arm actuated by the pneumatic muscles from (16) is described by

$$\begin{aligned}\dot{x}_1&=x_2\\ \dot{x}_2&=\bar{a}_A\Delta p^2-f(x_1,x_2,b_B(t))\Delta p\\ &\quad+h(x_1,x_2,b_E(t))\\ y&=x_1\end{aligned} \quad (18)$$

where $(x_1,x_2)\in(-\frac{\pi}{2},\frac{\pi}{2})\times\Re$ is the state, $\Delta p\in\Re$ and $y\in\Re$ are the system input and output respectively; $b_B:\Re\to\Re$ and $b_E:\Re\to\Re$ are functions which represent an uncertain time-varying parameters. From (15), it is obvious that there exists an *unknown* constant $\theta>0$, such that

$$|b_B(t)|\le\theta \text{ and } |b_E(t)|\le\theta \quad (19)$$

We are interested in the problem of global output tracking of the uncertain nonlinear system (18) under the following assumptions.

Assumption 1: There exists an *unknown* constant $M\ge 0$ such that a C^1 reference signal $y_r(t)$ satisfies

$$|y_r(t)|\le M \text{ and } |\dot{y}_r(t)|\le M \quad \forall t\ge 0 \quad (20)$$

Assumption 2: $\bar{a}_A$ is small. Hence, the term $\bar{a}_A\Delta p^2$ can be neglected.

Assumption 3: There exists an unknown real number f_m satisfying

$$0<f_m\le f\left(q,\dot{q},b_B(t)\right) \quad (21)$$

The problem of *adaptive output tracking* is formulated as follows. Let $y_r(t) \in C^1$ be a C^1 reference signal satisfying A1. For any $\varepsilon > 0$, find, if possible, an adaptive output tracking controller of the form

$$\begin{aligned} \dot{K} &= \eta(x_1, x_2, y_r(t)), \quad K \in \Re \\ u &= \mu(x_1, x_2, K, y_r(t)) \end{aligned} \tag{22}$$

such that

a) the state (x_1, x_2) of closed-loop system (18) and (22) is well-defined on $[0,+\infty)$ and globally bounded;

b) for every $[x_1(0), x_2(0)]^T \in \Re^2$, there is a finite time $T>0$ such that the output of the closed-loop system (18) and (22) satisfies

$$|y(t) - y_r(t)| < \varepsilon \quad \forall t \geq T > 0 \tag{23}$$

3.2 Adaptive Controller Design

The monotone adaptive control scheme in [11] and [12] are modified for the system (18). First, we define a change of coordinates by $e = x_1 - y_r$ and $\bar{e} = x_2 = \dot{x}_1$. Then the system (18) can be written as

$$\begin{aligned} \dot{e} &= \bar{e} - \dot{y}_r \\ \dot{\bar{e}} &= \bar{a}_A \Delta p^2 - f(x_1, x_2, b_B(t))\Delta p \\ &\quad + h(x_1, x_2, b_B(t)) \\ y &= x_1 \end{aligned} \tag{24}$$

Consider a Lyapunov function

$$V(e, \xi) = \frac{1}{2}e^2 + \frac{1}{2f_m}\xi^2 \tag{25}$$

where $\xi = \bar{e} + (1+K)e$ and the monotone non-decreasing function, , is governed by

$$\dot{K} = \begin{cases} sat_\beta\left(|y - y_r| - \dfrac{\varepsilon}{2}\right), & |y - y_r| \geq \dfrac{\varepsilon}{2} \\ 0, & |y - y_r| < \dfrac{\varepsilon}{2} \end{cases}$$

with $K(0) = 1$, $\forall \beta > 0$ (26)

The saturation function $sat_\beta(s) \in \Re$ is defined by

$$sat_\beta(s) = \begin{cases} s, & |s| \leq \beta \\ \operatorname{sgn}(s)\beta, & |s| > \beta \end{cases} \quad \forall s \in \Re$$

Then the time derivative of equation (25) along the system (24) satisfies

$$\begin{aligned} \dot{V} &= e\dot{e} + \frac{1}{f_m}\xi\dot{\xi} \\ &= e(\bar{e} - \dot{y}_r) + \frac{1}{f_m}\xi\left(\dot{\bar{e}} + (1+K)\dot{e} + \dot{K}e\right) \\ &= e(\bar{e} - \dot{y}_r) - \xi\frac{f(\cdot)}{f_m}\Delta p + \frac{1}{f_m}\xi h(\cdot) \\ &\quad + \frac{1}{f_m}\xi\left((1+K)\dot{e} + \dot{K}e\right) \end{aligned} \tag{27}$$

Using A1, (19) and the completion of square, it can be shown that

$$\begin{aligned} e(\bar{e} - y_r) &\leq \left(e\bar{e} + |e|M\right) \\ &\leq \left(e\bar{e} + Ke^2 + \frac{M^2}{4K}\right) \\ &= \left(-e^2 + e\xi + \frac{M^2}{4K}\right) \\ &\leq -\frac{e^2}{2} + \frac{\xi^2}{2} + \frac{\Theta_1(M)}{K} \end{aligned} \tag{28}$$

$$\begin{aligned} \frac{1}{f_m}\xi h(\cdot) &= \frac{1}{f_m}\xi\left\{\frac{b_B(t)\dot{q} + a_F q + a_G - mg\cos q}{ml_c^2 + I}\right\} \\ &\leq \frac{|\xi|\{\theta|x_2| + |a_F||x_1| + |a_G| + |mg|\}}{f_m(ml_c^2 + I)} \\ &\leq \frac{|\xi|\{\theta|\bar{e}| + |a_F||e| + |a_F|M + |a_G| + |mg|\}}{f_m(ml_c^2 + I)} \\ &\leq \xi^2\left(K\bar{e}^2 + Ke^2 + K\right) \\ &\quad + \frac{\Theta_2(\theta, M, f_m, a_F, a_G, m, g)}{K} \end{aligned} \tag{29}$$

where

$\Theta_1(M)=\frac{M^2}{4}\geq 0$ and

$\Theta_2(\cdot)=\frac{\theta^2+a_F^2+\left(|a_F|M+|a_G|+|mg|\right)^2}{4f_m^2\left(ml_c^2+I\right)^2}\geq 0$

are unknown constants.

Similarly, it can be shown that

$$\begin{aligned}\frac{1}{f_m}\xi\left((1+K)\dot{e}+K\dot{e}\right)&\leq\frac{1}{f_m}|\xi|\left(2K|\dot{e}|+\beta|e|\right)\\&\leq\frac{1}{f_m}|\xi|\left(2K\left(|\bar{e}|+M\right)+\beta|e|\right)\\&\leq\frac{1}{f_m}\xi^2\left(K^3\bar{e}^2+K^3+K\dot{e}^2\right)\\&\quad+\frac{\Theta_3(M,f_m,\beta)}{K}\end{aligned}\tag{30}$$

where $\Theta_3(\cdot)=\frac{1}{f_m^2}\left(\frac{4+4M^2+\beta^2}{4}\right)\geq 0$ is an unknown constant.

Substitute (28), (29) and (30) into (27). Hence,

$$\begin{aligned}\dot{V}&\leq-\frac{e^2}{2}+\frac{\xi^2}{2}+\frac{\Theta_1(M)}{K}-\xi\frac{f(\cdot)}{f_m}\Delta p\\&\quad+\xi^2\left(K\bar{e}^2+K\dot{e}^2+K\right)+\frac{\Theta_2(\cdot)}{K}\\&\quad+\xi^2\left(K^3\bar{e}^2+K^3+Ke^2\right)+\frac{\Theta_3(\cdot)}{K}\\&\leq-\frac{e^2}{2}+\frac{\xi^2}{2}-\xi\frac{f(\cdot)}{f_m}\Delta p\\&\quad+\xi^2\left(2K^3\bar{e}^2+2Ke^2+2K^3\right)+\frac{\Theta}{K}\end{aligned}\tag{31}$$

where the unknown constant $\Theta=\Theta_1(\cdot)+\Theta_2(\cdot)+\Theta_3(\cdot)$ is independent of the K.

With the choice of the controller

$$\Delta p=\xi\left(1+2K^3\bar{e}^2+2Ke^2+2K^3\right)\tag{32}$$

Then, we have

$$\begin{aligned}\dot{V}&\leq-\frac{e^2}{2}+\frac{\xi^2}{2}\\&\quad-\xi^2\frac{f(\cdot)}{f_m}\left(1+2K^3\bar{e}^2+2Ke^2+2K^3\right)\\&\quad+\xi^2\left(2K^3\bar{e}^2+2Ke^2+2K^3\right)+\frac{\Theta}{K}\end{aligned}\tag{33}$$

From A3, together with the fact that $-\xi^2\left(1+2K^3\bar{e}^2+2Ke^2+2K^3\right)\leq 0$, then (33) can be reduced as

$$\begin{aligned}\dot{V}&\leq-\frac{e^2}{2}-\frac{\xi^2}{2}+\frac{\Theta}{K}\\&\leq-bV+\frac{\Theta}{K}\end{aligned}\tag{34}$$

where $b=\min\{1,f_m\}>0$

In the remaining part of the proof, we show that all states $(e,\bar{e},K)$ of the closed-loop system (24), (32) and (26) are bounded and well-defined on $[0,+\infty)$. Moreover, given any $\varepsilon>0$, there exists a finite time T_ε such that the tracking error $|y-y_r|\leq\varepsilon,\ \forall t\geq T_\varepsilon$.

Using eq. (34), we obtain

$$\dot{V}\leq-bV+\Theta\tag{35}$$

which implies that (e,ξ,K) are well-defined on $[0,+\infty)$ and (e,ξ) is bounded. The compact set $\Omega=\left\{e,\xi\,|\,V(e,\xi)\leq a,\forall a\geq\frac{\Theta}{b}\right\}$ is invariant, since V is positive definite and proper and $\dot{V}$ is negative semi-definite $\forall e,\xi\in\Omega$. To show that $K(t)$ is bounded, we use a contradiction argument. Suppose that the monotone non-decreasing function $K(t)$ is unbounded. Then there must exist a finite time T^* such that

$$K(t)\geq\frac{\Theta}{\varepsilon^*},\ \varepsilon^*=\frac{b\varepsilon^2}{16}\quad\forall t\geq T^*$$

and (34) becomes

$$\dot{V} \le -bV + \varepsilon^* \quad \forall t \ge T^*$$

Consequently,

$$V(t) \le e^{-b(t-T^*)}\left(V(T^*) - \frac{\varepsilon^*}{b}\right) + \frac{\varepsilon^*}{b} \quad \forall t \ge T^* \tag{36}$$

This implies that there exists another finite time T_1 such that

$$\frac{|y - y_r|^2}{2} = \frac{e^2}{2} \le V(t) \le \frac{2\varepsilon^*}{b} = \frac{\varepsilon^2}{8} \quad \forall t \ge T_1$$

which contradicts the assumption that $K(t)$ is unbounded since

$$\dot{K}(t) = 0 \qquad \forall t \ge T_1 .$$

Since $K(t)$ is bounded, we can conclude that all of the states $(e, \bar{e}, K)$ of equations (24), (32) and (26) are also bounded and well-defined. Hence, from A1, the closed-loop system trajectories generated by equations (24), (32) and (26) are well-defined and bounded on $[0, +\infty)$.

In addition, the integral of $\dot{K}(t)$ evaluated from zero to infinity exists and it finite, that is

$$\lim_{t\to\infty} \int_0^t \dot{K}(\tau)d\tau = K(\infty) - K(0) < +\infty$$

Since $\dot{K}(t)$ is uniformly continuous, it follows from *Barbalat' s lemma* that

$$\lim_{t\to\infty} \dot{K}(t) = 0$$

This, together with equation (26), implies the existence of a finite time T_ε satisfying

$$|y - y_r| \le \varepsilon \qquad t \ge T_\varepsilon > 0$$

4. SIMULATION RESULTS

We investigate the closed-loop system behaviors of our adaptive control. The one-link planar robot arm studied here is similar to those in Figure 4. The closed-loop system is simulated with the physical parameters of the arm as follows, m = 1 slug, l = 20 in., l_c =10 in., r = 2 in. and the number of muscle pairs n = 6. All of the simulation were performed with the initial conditions, $[x_1(0), x_2(0)]^T = [1,1]^T$, ε = 0.1 rad., β = 10 and the nominal pressures, P_{0i1} = 40 psi. and P_{0i1} = 60 psi.

In the simulations, we restricted the internal pressure in each muscle within the range, $0 \le P \le 130$ psi. since in a real system, the internal pressure can not go below zero and the parameters of the muscles using in here are only valid in this range. In addition, we use the full nonlinear model which includes the term $\bar{a}_A \Delta p^2$ in all simulations.

We studied three cases of the muscle parameter sets as shown in table 1. The nominal parameters are the ones studied in [4]. The other two sets of coefficients represent 50% increase and 50% decrease of muscle coefficients. *Case A* represents the system under a normal condition and has a matching pair of muscle groups. *Case B* and *Case C* represent the cases when the system has a mismatch pair of muscle groups or undergoes severe changes of muscle properties.

Table 1. Case studies for investigate tracking performance.

Case	Bicep	Tricep
A	Nominal	Nominal
B	+50%	-50%
C	-50%	+50%

We chose two different types of reference trajectories. The first one was a sum of sinusoidal signals,

$$y_r = 0.5\sin(0.1\pi \cdot t) + 0.8\sin(0.05\pi \cdot t) + 0.5\sin(0.2\pi \cdot t) \quad \text{rad.} \tag{37}$$

The other was a pseudo-square wave signal,

$$y_r = \begin{cases} -1.2 & ,\sin(0.1\pi \cdot t) \le -1.2 \\ 1.5\sin(0.08\pi \cdot t) & ,|\sin(0.1\pi \cdot t)| < 1.2 \\ 1.2 & ,\sin(0.1\pi \cdot t) \ge 1.2 \end{cases} \text{ rad.} \quad (38)$$

We performed the simulations for 40,000 sec and at t = 30,000 s., we switch the reference signal from the sum of sinusoidal signals to the pseudo-square wave signal. The simulation results in three cases are shown in Figure 5-10.

The tracking performance and tracking error in *Case A*, *B* and *C* are shown in Figure 5, 7 and 9 respectively. All of the cases demonstrated that the tracking error would eventually be within the prescribed error $\varepsilon = 0.1$ rad. after a finite time.

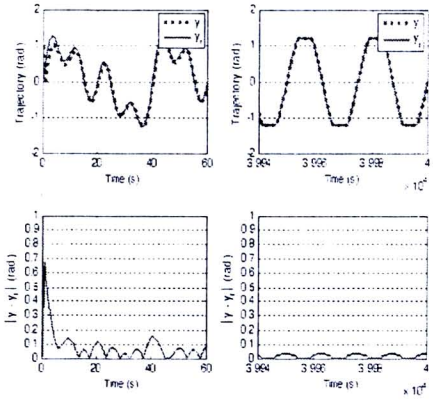

Figure 5. Joint angle trajectory and the error in *Case A*.

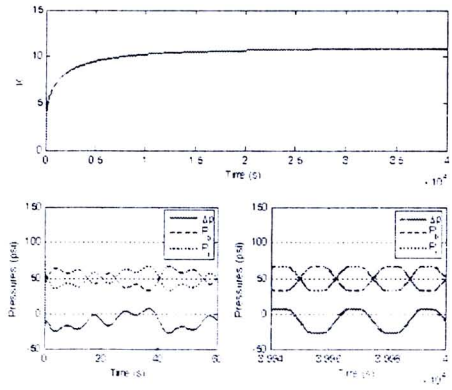

Figure 6. Adaptive gain and Pressures in *Case A*.

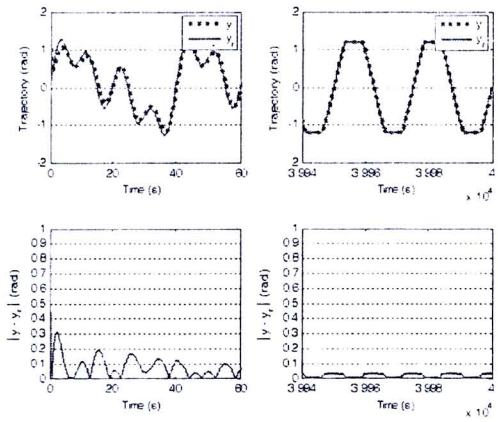

Figure 7. Joint angle trajectory and the error in *Case B*.

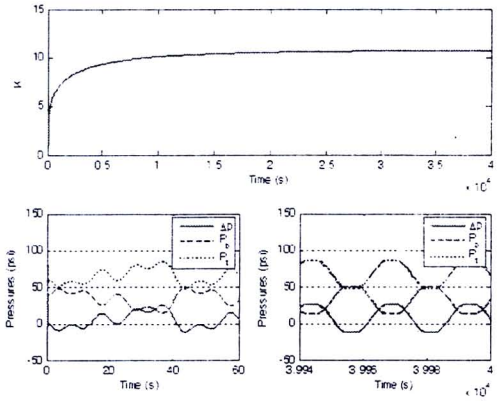

Figure 8. Adaptive gain and Pressures in *Case B*.

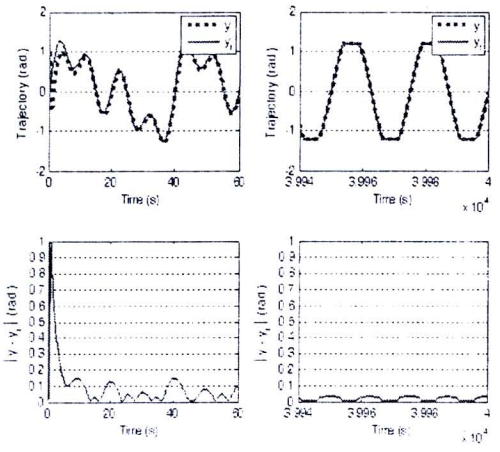

Figure 9. Joint angle trajectory and the error in *Case C*.

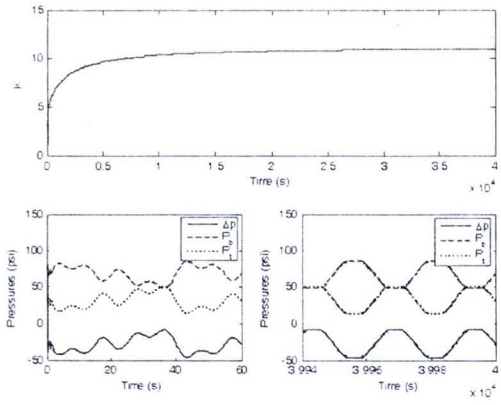

Figure 10. Adaptive gain and Pressures in *Case C.*

5. CONCLUSIONS

In this paper, we develop an adaptive controller for a one-link robot arm actuated by pneumatic muscles under the conditions that all physical parameters of the system are *unknown*. Moreover, the bound of uncertain time-varying parameter are not known a priori.

The proposed control law can regulate the joint angle to follow any C^1 trajectory. The closed-loop states are globally bounded and the angle error will be within any nonzero prescribed error in a finite time. We demonstrate the performance and characteristic by simulations. The simulations show that our adaptive control scheme can achieve angle tracking even under severe changes of system parameters.

7. REFERENCES

[1] Chou C.P., and Hannaford B., Static and Dynamic Characteristics of McKibben Pneumatic Artificial Muscles, *Proc. IEEE International Conference on Robotics and Automation*, San Diego, CA, USA, May 1994.

[2] Chou C.P., and Hannaford B., Measurement and Modeling of McKibben Pneumatic Artificial Muscles , *IEEE Trans. on Robotics and Automation*, 1996; **12**:90-102.

[3] Tondu B., and Lopez P. , Modeling and Control of McKibben Pneumatic Artificial Muscle Robot Actuators, *IEEE Control Systems Magazine*, 2000; **20**:15-38.

[4] Reynolds D.B., Repperger D.W., Philips C.A., and Bandry G., Dynamic characteristics of pneumatic muscle, *Computers in Biology and Medicine*. Submitted.

[5] Reynolds D.B., Repperger D.W., Phillips C.A., and Bandry G., Modeling the Dynamic characteristics of pneumatic muscle, *Ann. Biomed. Eng.*, 2003; **31**: 310–317.

[6] Lilly J., Adaptive tracking for pneumatic muscle actuators in bicep and tricep configurations *IEEE Trans. Neural Systems Rehabilitation Eng.*, 2003; **11**: 333-339.

[7] Lilly J., and Quesada P., A Two-Input Sliding-Mode Controller for a Planar Arm Actuated by Four Pneumatic Muscle Groups, *IEEE Trans. Neural Syst. Rehabil. Eng.*, 2004; **12**: 349–359.

[8] Lilly J., and Yang L., Sliding Mode Tracking for Pneumatic Muscle Actuators in Opposing Pair Configuration, *IEEE Trans. Control Systems Technology*, 2005; **13**: 550-558.

[9] Chang X., and Lilly J., 2003, The Dynamics of PM Arm and Its Control [Online], *http://louisville.edu/~x0chan01/res/pms.htm*

[10] Lilly J., and Chang X., A Fuzzy Model Predictive Controller for a Planar Arm Actuated by Four Pneumatic Muscle Group [Online], Available *http://louisville.edu/~x0chan01/res/pms.htm*

[11] Lin W., and Pongvuthithum R., Adaptive output tracking of inherently nonlinear systems with nonlinear parameterization, *IEEE Trans. Automatic Control*, 2003; **48**: 1737-1349.

[12] Pongvuthithum R., Veres S.M., Gabriel S.B., and Rogers E., Universal adaptive control of satellite formation flying, *International Journal of Control*, 2005; **78**: 45-52.

Draft submitted to IEEE Transaction on Neural Systems and Rehabilitation Engineering

Adaptive Control for Multi-Link Robots Actuated by Pneumatic Muscles

T. Karnjanaparichat and R. Pongvuthithum

Department of Mechanical Engineering,
Faculty of Engineering,
Chiang Mai University,
Chiang Mai 50200, Thailand.

Abstract

Pneumatic muscles or McKibben muscles are lightweight and very high power-to-weight ratio actuators. Their construction are simple inheritly soft and compliant. Hence, they are suitable to use in the environment when there are interactions between men and machines. However, controls of various mechanical systems actuated by pneumatic muscles are facing various problems. The parameters of the muscles are nonlinear and time varying due to temperature changing and the deterioration of the pneumatic muscle materials when the muscles are used for an extended period of time. To solve the control problems of pneumatic muscle system, the controller has to be able to adapt to any chance in system parameters and if possible, is independent of the system parameters.

In this paper, we study the problem of adaptive position tracking for any $\mathbf{C}^1$ signal of a multi-link robot driven by two opposing pneumatic muscle groups. The proposed adaptive control law is independent of the system parameters (such as load at the end of the robot, the pneumatic muscle coefficients, the lengths, the moments of inertia and etc.) and the bound of reference signal and its derivative are unknown. All joint angle errors will be within the prescribed error in finite time.

Keyword: Pneumatic Muscle; Adaptive Control; Multi-Link Robot

1 Introduction

The artificial pneumatic muscles are used in various applications such as robotics, bio-robotics, biomechanics, artificial limb replacements and many industry tasks. The advantages of the pneumatic muscles are the ease of use compared to standard pneumatic cylinders and their simple construction. The pneumatic muscles are also soft, lightweight and have a high power/force-to-weight ratio. In addition, the pneumatic muscles can be twisted axially i.e. not aligned and bended. These features make pneumatic muscles a major interest for the researchers and hobbyists.

The mathematical models of pneumatic muscle have been developed in two main different ways, dynamics and static models. Chou and Hannaford [1] and [2], and Tondu and Lopez [3] developed static models by using virtual work to find the relation of force, pressure and lengths of muscle whereas the dynamics models have been developed by Reynolds et al. [4] and [5]. They modeled the muscles consisting of three elements, a spring, a damping and a contractile in a parallel arrangement. Furthermore, Cai and Yamaura [11] considered some factors into tradition static models ([1],[2] and [3]) and many researches [14],[15] and [16] integrated air flow of a valve into the static model. However, this paper focuses on the dynamics model due to it have a simpler structure of the muscle comparing to the static model.

The control of pneumatic muscle is difficult due to the physical parameters being nonlinear and time-varying. Therefore, many researchers have proposed control schemes for solving problems of

the uncertain mechanical systems actuated by pneumatic muscles. For example, Lilly [6] proposed a model reference adaptive controller as based on sliding-mode for a planar robot arm actuated by pneumatic muscles. Tonietti and Bicchi [13] developed a model reference adaptive controller for a n-DOF robot arm actuated by pneumatic muscles. The adaptive controllers ([6] and [13]) require the exact forms of the nonlinear terms and the system mechanical properties, e.g. the links' mass, lengths and inertias. In [7], Lilly and Quesada developed a robust controller as based on sliding-mode for a two-link arm actuated by pneumatic muscles. Lilly and Yang [8] developed a robust controller as based on sliding-mode for a pneumatic muscle actuator. Cai and Yamaura [11] and Cai and Dai [12] developed a robust controller as based on sliding-mode for a pneumatic muscle actuator. Zhang at el. [14] developed an adaptive robust control of a one-link joint actuated by pneumatic muscles. Zhu at el. [15] and Tao at el. [16] developed an adaptive robust controller for posture trajectory tracking of a parallel manipulator driven by three pneumatic muscles. Most robust control techiques ([7] ,[8], [11], [12], [14], [15] and [16]) are necessary to know the bounds of some parameters or terms in system. Furthermore, the controller design ([6], [7] and [8]) is based on sliding-mode, chattering can occur due to the controller being a discontinuous function. Lilly and Chang, [9] and [10], developed Fuzzy predictive controller for a two-link arm actuated pneumatic muscles. A fuzzy model was developed based on linearized model around operating point on state space, therefore all of system parameters must be known precisely.

For pneumatic muscles, muscle property changes due to temperature changes and the deterioration of the pneumatic muscle materials when the muscles are in use for an extended period of time are common. Hence we should develop a controller that is independent of all system parameters and can adapt the system parameter changes. In this paper, we will focus on designing an adaptive control scheme for the multi-link robots actuated by pneumatic muscles. The proposed control scheme is based on a monotone adaptive control studied in [17] and [18]. The remaining of the paper is organized as follows. Section 2 contains concepts of pneumatic muscle model, the some properties of rigid robot and setup the dynamics of multi-link robot actuated by pneumatic muscles. Design methodology of the monotone adaptive control scheme is presented in Section 3. Simulation example results in the two-link planar arm case demonstrated the performance of our control law are in Section 4. Finally, conclusions are drawn in Section 5.

2 Dynamics of Multi-Link Arm Actuated by Pneumatic Muscles

2.1 Dynamics of pneumatic muscle actuator

Typically, a pneumatic muscle is modeled by three elements, a spring a damping and a contractile, connecting in parallel, see Fig. 1. From [4] and [5], the total force exerted by the muscle on the mass is

$$R = F(P) - B(P)\dot{y} - K(P)y \tag{2.1}$$

where F is the force exerted by the contractile element, B is the damping coefficient and K is the spring coefficient. Using data from experiments, the coefficients were formulated as polynomial functions of the input pressure of the muscle.

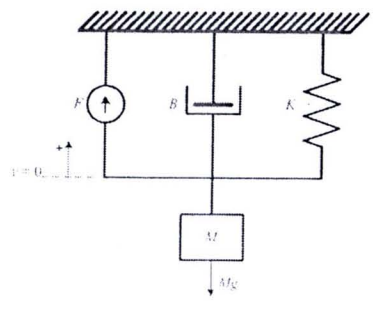

Figure 1: A three-element model of the pneumatic muscle.

To find the coefficient functions of the three-elements, the muscle was hung vertically with a mass attached at the lower end. Then, the muscle was inflated and held at various constant P. Let $y = 0$ be the position of the mass when the muscle is completely deflated see Fig. 2. The position y and the values of the three coefficients were determined by perturbing the load at each constant P. Under the assumption that the spring and damping coefficient functions determined by perturbation of the load at constant P are the same functions as obtained in the dynamic condition, the coefficient functions were formulated by the least square method.

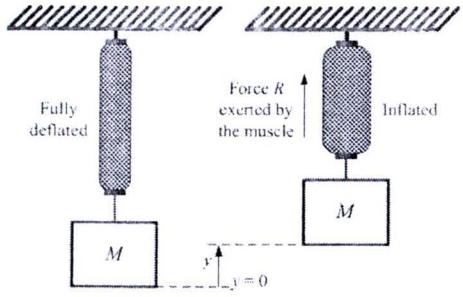

Figure 2: The pneumatic muscle is actuating a mass.

According to [4], the coefficient functions of the three elements are given as:

$$\begin{aligned} K(P) &= K_0 + K_1 P \\ &= 32.58 + 1.209P \qquad (2.2) \\ B(P) &= B_0 + B_1 P \\ &= 5.748 + 0.2719P \quad \text{(Inflation)} \qquad (2.3) \\ B(P) &= B_0 - B_1 P \\ &= 3.41 - 0.0316P \quad \text{(Deflation)} \qquad (2.4) \\ F(P) &= F_1 P - F_2 P^2 \\ &= 3.77P - 0.0138P^2 \qquad (2.5) \end{aligned}$$

The coefficients in (2.2)-(2.5) are applicable for pressures in the range $0 \leq P \leq 130$ psi.

Consider a pneumatic muscle pair putting into antagonism similar to an actuator based on the physiological model of the bicep-tricep system in Fig. 3. The muscle pairs are connected by means of a chain driving a sprocket. The group of right muscles is not necessary to have the same muscle coefficients as the group of left muscles. The force difference between the agonist and the antagonist generates a positive or negative torque.

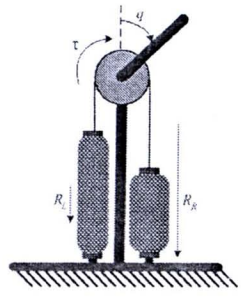

Figure 3: The pneumatic muscle pairs tied together around a sprocket.

Assume that the n pneumatic muscle pairs tied together around a sprocket of radius r as in Fig. 3. with the connecting line rigidly attached to the sprocket to prevent slipping. The torque produced to the sprocket by the muscle pairs is

$$\tau = \tau_R - \tau_L = (R_R - R_L)r \qquad (2.6)$$

where R_R and R_L are the total force exerted by an individual group of right and left muscles respectively. When the force $R_R > R_L$, then the torque exerted on the joint is clockwise and vice versa. From (2.1), we have

$$R_R = n(F_R - B_R\dot{x}_R - K_R x_R) \tag{2.7}$$
$$R_L = n(F_L - B_L\dot{x}_L - K_L x_L) \tag{2.8}$$

where x_R is the length of right muscles and x_L is the length of left muscles. Substitute (2.7) and (2.8) into (2.6), then the total torque delivered to the sprocket is given by

$$\tau = n(F_R - B_R\dot{x}_R - K_R x_R - F_L + B_L\dot{x}_L + K_L x_L)r \tag{2.9}$$

where F_R, K_R and B_R depend on the input pressure of right muscles and F_L, K_L and B_L depend on the input pressure of left muscles.

A joint angle of $q = \pi$ rad. corresponds to the left muscles being fully extended and the right fully contracted, and $q = -\pi$ rad. corresponds to the left muscles being fully contracted and the right fully extended. Therefore, the muscle lengths x_R and x_L can be expressed in terms of q as

$$x_R = (\pi + q)r \tag{2.10}$$
$$x_L = (\pi - q)r \tag{2.11}$$

Let the internal pressure of the right muscles P_R and left muscles P_L be

$$P_R = P_{0R} - \Delta p \tag{2.12}$$
$$P_L = P_{0L} + \Delta p \tag{2.13}$$

where P_{0R} and P_{0L} are arbitrary positive nominal constant pressures and Δp is a control input. With the definition (2.12)-(2.13), the antagonist pairs become a single-input system with input Δp.

From (2.9)-(2.13) and the coefficient functions (2.2)-(2.5), the torque can be written as

$$\tau = a_A^2\Delta p^2 - (b_B(t)\ddot{q} + a_c\dot{q} + a_D q)\Delta p + b_E(t)\ddot{q} + a_F\dot{q} + a_G q \tag{2.14}$$

where

$$a_A = n(F_{2L} - F_{2R})r \tag{2.15}$$
$$b_B(t) = \begin{cases} -n(B_{1Li} + B_{1Rd})r^2 & ,\dot{q} < 0 \\ 0 & ,\dot{q} = 0 \\ n(B_{1Ld} + B_{1Ri})r^2 & ,\dot{q} > 0 \end{cases} \tag{2.16}$$
$$a_C = n(K_{1R} - K_{1L})r^2 \tag{2.17}$$
$$a_D = n(2F_{2R}P_{0R} - F_{1R} + 2F_{2L}P_{0L} - F_{1L} + rK_{1R}\pi + rK_{1L}\pi)r \tag{2.18}$$
$$b_E(t) = \begin{cases} -n(B_{0Li} + B_{1Li}P_{0L} + B_{0Rd} - B_{1Rd}P_{0R})r^2 & ,\dot{q} < 0 \\ 0 & ,\dot{q} = 0 \\ -n(B_{0Ld} - B_{1Ld}P_{0L} + B_{0Ri} + B_{1Ri}P_{0R})r^2 & ,\dot{q} > 0 \end{cases} \tag{2.19}$$
$$a_F = -n(K_{1L}P_{0L} + K_{1R}P_{0R} + K_{0L} + K_{0R})r^2 \tag{2.20}$$
$$a_G = -n(F_{2R}P_{0R}^2 - F_{1R}P_{0R} - F_{2L}P_{0L}^2 + F_{1L}P_{0L} + rK_{1R}P_{0R}\pi + rK_{0R}\pi - rK_{1L}P_{0L}\pi - rK_{0L}\pi)r \tag{2.21}$$

The coefficients in (2.15)-(2.21). R and L subscripts indicate the coefficients of right and left muscles respectively. The subscripts, i and d, on the coefficient B denote whether the muscles are being inflated and deflated respectively.

2.2 Dynamics of rigid robot and some properties

In the absence of friction and disturbances, the dynamics of a multi-link rigid robot is given by the *Euler-Lagrange* equation

$$D(q)\ddot{q} + C(q,\dot{q})\dot{q} + f(q) = \tau \tag{2.22}$$

where $q \in \mathbb{R}^n$ is the generalized coordinate vector of n links, $D(q)$ is the inertia matrix which is positive definite and symmetric, $C(q,\dot{q})$ accounts for the *coriolis/centrifugal* term, $g(q)$ is the gravity vector, and τ is the generalized torque acting on the joints.

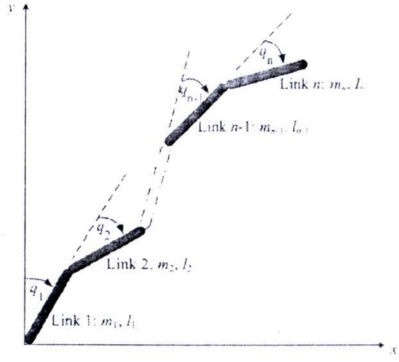

Figure 4: Multi link robot configuration

For revolute joints, the only occurrences of the joint variables q_i are as $\sin(q_i)$ and $\cos(q_i)$, where $i = 1, \ldots. n$.The rigid robot dynamics in (2.22) posses a number of some properties that facilitate analysis and controller design. These are

Property 2.1 The inertia matrix $D(q)$ is symmetric, positive definite, and bounded so that

$$\mu_m I \leq D(q) \leq \mu_M I. \quad \forall q(t). \tag{2.23}$$

Then, the inverse of inertia matrix is bounded, since

$$\frac{1}{\mu_M} I \leq D^{-1}(q) \leq \frac{1}{\mu_M} I. \tag{2.24}$$

Moreover, the bounded of inertia matrix may also be expressed as

$$\mu_m \leq \| D(q) \| \leq \mu_M. \tag{2.25}$$

Likewise, the bounded of the inverse inertia matrix is

$$\frac{1}{\mu_M} \leq \| D^{-1}(q) \| \leq \frac{1}{\mu_M}. \tag{2.26}$$

Property 2.2 The *coriolis/centrifugal* term $C(q,\dot{q})\dot{q}$ is bounded $C_M \geq 0$ so that

$$\| C(q,\dot{q})\dot{q} \leq C_M \| \dot{q} \|^2. \tag{2.27}$$

Property 2.3 The gravity vector are bounded $F_M \geq 0$ so that

$$\| f(q) \| \leq F_M. \tag{2.28}$$

2.3 Dynamics of multi-link robots actuated by pneumatic muscles

In this section, the general dynamics equations of multi-link robots actuated by pneumatic muscles are summarized. From Section 2.2, the dynamics of the pneumatic muscle actuators that drive the n-link are given by the n decoupled equations as

$$\tau_i = a_{Ai}\Delta p_i^2 - h_i(q, \dot{q}, b_{Bi}(t))\Delta p_i + b_{Ei}(t)\dot{q}_i + a_{Fi}q_i + a_{Gi}, \quad i = 1, ..., n. \tag{2.29}$$

where $h_i(\cdot) = b_{Bi}(t)\dot{q}_i + a_{Ci}q_1 + a_{Di}$ is a function, a_{Ai}, a_{Ci}, a_{Di}, a_{Fi} and a_{Gi} are constants, $b_{Bi} : \mathbb{R} \to \mathbb{R}$ and $b_{Ei} : \mathbb{R} \to \mathbb{R}$, $i = 1, ..., n$, are uncertain time-varying functions which can be written in form

$$\begin{aligned} b_{Bi}(t) &= \eta_{Bi} + \mu_{Bi}sgn(\dot{q}_i) \\ b_{Ei}(t) &= \eta_{Ei} + \mu_{Ei}sgn(\dot{q}_i) \end{aligned}$$

where η_{Bi} and η_{Ei} are constants. μ_{Bi} and μ_{Ei} are constants which are the Coulomb sliding friction. Then $b_{Bi}(t)$ and $b_{Ei}(t)$ are bounded by an *unknown* constants $\theta_{Bi} > 0$ and $\theta_{Ei} > 0$ respectively, such that

$$|b_{Bi}(t)| \leq \theta_{Bi} \quad \text{and} \quad |b_{Ei}(t)| \leq \theta_{Ei} \tag{2.30}$$

To define $q = [q_1, ..., q_n]^T$, hence it is common to write (2.29) in the matrix from as

$$\tau = A_A\bar{p} - H(q, \dot{q}, b_{Bi})\Delta p + B_E(t)\dot{q} + A_F q + \hat{a}_G \tag{2.31}$$

where

$$\begin{aligned} A_A &= diag\{a_{A1}, ... a_{An}\} && (2.32) \\ \bar{p} &= [\Delta p_1^2, ..., \Delta p_n^2]^T && (2.33) \\ \Delta p &= [\Delta p_1, ..., \Delta p_n]^T && (2.34) \\ H(q, \dot{q}, b_{Bi}(t)) &= diag\{h_1(\cdot), ..., h_n(\cdot)\} && (2.35) \\ B_E(t) &= diag\{b_{E1}(t), ..., b_{En}(t)\} && (2.36) \\ A_F &= diag\{a_{F1}(t), ... a_{Fn}(t)\} && (2.37) \\ \hat{a}_G &= [a_{F1}, ..., a_{Fn}]^T && (2.38) \end{aligned}$$

Finally, the general form of the rigid robot dynamics in (2.22) are combined with (2.31)-(2.38), we can arrive at the following model for the a multi-link robot actuated by the pneumatic muscles as

$$\ddot{q} = D^{-1}(q)\left\{A_A\bar{p} - H(q, \dot{q}, b_{Bi}(t))\Delta p + B_E(t)\dot{q} + A_F q + \hat{a}_G - C(q, \dot{q})\dot{q} - f(q)\right\} \tag{2.39}$$

where $q \in \mathbb{R}^n$ is a state vector, $\Delta p \in \mathbb{R}^n$ is the system input vector.

All $b_{Ei}(t)$ are the elements of the diagonal matrix $B_E(t)$, then $B_E(t)$ bounded by an *unknown* constant $\Theta_E = \max\{\theta_{Ei}\} > 0$, such that

$$\| B_E(t) \| \leq \Theta_E \tag{2.40}$$

Moreover, A_F is a constant diagonal matrix bounded by an *unknown* constant $\Theta_F = \max\{|a_{Fi}|\} > 0$ and $\hat{a}_G$ is a constant vector bounded by an *unknown* constant $\Theta_G = \sqrt{\sum_{i=1}^{n} a_{Gi}^2} > 0$, such that

$$\| A_F \| \leq \Theta_F \quad \text{and} \quad \| \hat{a}_G \| \leq \Theta_G \tag{2.41}$$

3 Adaptive Position Tracking Control

3.1 Problem statement

The problem of *adaptive position tracking* is formulated as follows. Given a constant $\varepsilon > 0$ and a bounded reference signal $q_r = [q_{1r}, ... q_{nr}]^T \in \mathbf{C}^1$ whose derivative is also bounded, find, if possible, an adaptive controller of the form

$$\begin{aligned} \dot{K} &= \eta(q, q_r(t)), \quad K \in \mathbb{R} \\ \Delta p &= \mu(q, K, q_r(t)), \quad \Delta p \in \mathbb{R}^n \end{aligned} \tag{3.42}$$

such that

a) the states of the closed-loop system (2.39) and (3.42) are well-defined on $[0, +\infty)$ and globally bounded;

b) there is a finite time $T_\varepsilon > 0$ such that the closed-loop system (2.39) and (3.42) trajectories satisfy

$$\| q(t) - q_r(t) \| < \varepsilon, \quad \forall t \geq T_\varepsilon > 0. \tag{3.43}$$

Throughout this system we make the following assumptions.

Assumption 3.1 The exists an unknown constant $M \geq 0$ such that the reference signal $q_r(t)$ satisfies

$$\| q_r(t) \| + \| \dot{q}_r(t) \| \leq M \tag{3.44}$$

Assumption 3.2 For all a_{Ai} is small. Hence, all of the terms of $a_{Ai}\Delta p_i^2$ can be neglect when $i = 1, ..., n$.

Assumption 3.3 There exists an unknown constants λ_i and λ, where $i = 1, ..., n$. Satisfying

$$0 < \lambda \leq \lambda_i \leq h_i(q, \dot{q}, b_{Bi}(t)), \quad \lambda \leq \min\{\lambda_i\} \tag{3.45}$$

3.2 Adaptive control scheme

The monotone adaptive control scheme in [17] and [18] are modified for the system (2.39). First, we define a change of coordinates by $e = [e_1, ..., e_n]^T$ and $\bar{e} = [\bar{e}_1, ..., \bar{e}_n]^T$. Then, the system (2.39) can be written as

$$\begin{aligned} \dot{e} &= \bar{e} - \dot{q}_r \\ \dot{\bar{e}} &= D^{-1}(q)\{A_A\bar{p} - H(q, \dot{q}, b_{Bi}(t))\Delta p + B_E(t)\dot{q} + A_F q + \hat{a}_G - C(q.\dot{q})\dot{q} - f(q)\} \end{aligned} \tag{3.46}$$

With this in mind, consider a Lyapunov function

$$V = \frac{1}{2}e^T e + \frac{\mu_M}{2\lambda}\xi^T\xi \tag{3.47}$$

where μ_M is the upper bound of the inertia matrix $D(q)$. To define $\xi_i = \bar{e}_i + (1 + K)e_i$ and the monotone non-decreasing function, $K(t) \geq 1$, is governed by

$$\dot{K} = \begin{cases} sat_\beta(\| q - q_r \| - \frac{\varepsilon}{2}) & , \| q - q_r \| \geq \frac{\varepsilon}{2} \\ 0 & , \| q - q_r \| < \frac{\varepsilon}{2} \end{cases} \tag{3.48}$$

and the saturation function $sat_\beta(s) \in \mathbb{R}$ is defined by

$$sat_\beta(s) = \begin{cases} s & , |s| \leq \beta \\ sgn(s)\beta & , |s| > \beta \end{cases} \tag{3.49}$$

Then, the time derivative of equation (3.47) along the trajectories of the system (3.46) satisfies

$$\begin{aligned} \dot{V} &= e^T\dot{e} + \frac{\mu_M}{\lambda}\xi^T\dot{\xi} \\ &= e^T\dot{e} - \frac{\mu_M}{\lambda}\xi^T D^{-1}(q)H(\cdot)\Delta p + \frac{\mu_M}{\lambda}\xi^T D^{-1}(q)\{B_E(t)\dot{q} + A_F q + \hat{a}_G - C(q.\dot{q})\dot{q} - f(q)\} \\ &\quad + \frac{\mu_M}{\lambda}\xi^T\{(1 + K)\dot{e} + \dot{K}e\} \end{aligned} \tag{3.50}$$

Using Assumption 3.1 and the completion of square, it is difficult to show that

$$\begin{aligned} e_1\dot{e}_1 &= e_1\bar{e}_1 - e_1\dot{q}_r \\ &\leq e_1\bar{e}_1 + |e_1|M \\ &\leq e_1\bar{e}_1 + Ke_1^2 + \frac{M^2}{4K} \\ &= -e_1^2 + e_1\xi_1 + \frac{M^2}{4K} \\ &\leq -\frac{e_1^2}{2} + \frac{\xi_1^2}{2} + \frac{M^2}{4K} \end{aligned}$$

Applying the same process to terms $i = 2, ..., n$, we have

$$e^T\dot{e} = \sum_{i=1}^{n} e_i\dot{e}_i \leq \sum_{i=1}^{n}\left(-\frac{e_i^2}{2} + \frac{\xi_i^2}{2}\right) + \frac{\Theta_1(n.M)}{K} \tag{3.51}$$

where $\Theta_1(n, M) = \frac{nM^2}{4} \geq 0$ is an unknown constant.

Using Assumption 3.1, (2.40), (2.41) and the completion of square, it can be shown that

$$\begin{aligned} \| B_E(t)\dot{q} + A_F q + \hat{a}_G \| &\leq \Theta_E \| \dot{q} \| + \Theta_F \| q \| + \Theta_G \\ &\leq \Theta_E \| \bar{e} \| + \Theta_F \| e \| + \Theta_F M + \Theta_G \end{aligned} \tag{3.52}$$

Using Property 2.2 and 2.3 of rigid robot dynamics, such that

$$\begin{aligned} \| -C(q,\dot{q})\dot{q} - f(q) \| &\leq C_M \| \dot{q} \|^2 + F_M \\ &= C_M \| \bar{e} \|^2 + F_M \end{aligned} \tag{3.53}$$

Let $\Psi(\cdot) = D^{-1}(q)\{B_E(t)\dot{q} + A_F q + \hat{a}_G - C(q,\dot{q})\dot{q} - f(q)\}$. According to (3.52), (3.53) and using Property 2.1, it can be shown that

$$\begin{aligned} \frac{\mu_M}{\lambda}\xi^T\Psi(\cdot) &\leq \frac{\mu_M}{\lambda} \| \xi \| \| D^{-1}(q) \| \| B_E(t)\dot{q} + A_F q + \hat{a}_G \| \\ &\quad + \frac{\mu_M}{\lambda} \| \xi \| \| D^{-1}(q) \| \| -C(q,\dot{q})\dot{q} - f(q) \| \\ &\leq \frac{\mu_M}{\lambda\mu_m} \| \xi \| (\Theta_E \| \bar{e} \| + \Theta_F \| e \| + \Theta_F M + \Theta_G) \\ &\quad + \frac{\mu_M}{\lambda\mu_m} \| \xi \| \left(C_M \| \bar{e} \|^2 + F_M\right) \\ &\leq \| \xi \|^2 \left(K \| e \|^2 + K \| \bar{e} \|^2 + K \| \bar{e} \|^4 + K\right) + \frac{\Theta_2(\cdot)}{K} \\ &:= \sum_{i=1}^{n} \xi_i^2 \rho(e, \bar{e}, K) + \frac{\Theta_2(\cdot)}{K} \end{aligned} \tag{3.54}$$

where $\Theta_2(\cdot) = (\frac{\mu_M}{\lambda\mu_m})^2 \left\{\frac{\Theta_E^2 + \Theta_F^2 + C_M^2 + (\Theta_F M + \Theta_G + F_M)^2}{4}\right\} > 0$ is an unknown constant.

To derive an upper bound on the terms involving K in (3.50), where using the fact that , we obtain

$$\begin{aligned} \frac{\mu_M}{\lambda}\xi_i\left\{(1+K)\dot{e}_i + \dot{K}e_i\right\} &\leq \frac{\mu_M}{\lambda}|\xi_i|\left\{(1+K)(|\bar{e}_i| + M) + \beta|e_i|\right\} \\ &\leq \frac{\mu_M}{\lambda}|\xi_i|\left(2K|\bar{e}_i| + 2KM + \beta|e_i|\right) \\ &\leq \xi_i^2\left(K^3\bar{e}_i^2 + K^3 + Ke_i^2\right) + \left(\frac{\mu_M}{\lambda}\right)^2 \frac{(4 + 4M^2 + \beta^2)}{4K} \end{aligned}$$

Applying the same process to the terms $i = 2, ..., n$, we have

$$\begin{aligned} \frac{\mu_M}{\lambda}\xi^T\left\{(1+K)\dot{e} + \dot{K}e\right\} &\leq \sum_{i=1}^{n} \xi_i^2\left(K^3\bar{e}_i^2 + K^3 + Ke_i^2\right) + \frac{\Theta_3(\cdot)}{K} \\ &:= \sum_{i=1}^{n} \xi_i^2\hat{\rho}_i(e_i, \bar{e}_i, K) + \frac{\Theta_3(\cdot)}{K} \end{aligned} \tag{3.55}$$

where $\Theta_3(\cdot) = n\,(\frac{\mu_M}{\lambda})^2 \left\{\frac{4 + 4M^2 + \beta^2}{4}\right\} > 0$ is an unknown constant.

Combining (3.51), (3.54) and (3.55) together, yields

$$\begin{aligned} \dot{V} &\leq \sum_{i=1}^{n}\left(-\frac{e_i^2}{2} + \frac{\xi_i^2}{2}\right) + \frac{\Theta_1(\cdot)}{K} - \frac{\mu_M}{\lambda}\xi^T D^{-1}(q)H(\cdot)\Delta p + \sum_{i=1}^{n} \xi_i^2\rho(e, \bar{e}, K) + \frac{\Theta_2(\cdot)}{K} \\ &\quad + \sum_{i=1}^{n} \xi_i^2\hat{\rho}_i(e_i, \bar{e}_i, K) + \frac{\Theta_3(\cdot)}{K} \\ \dot{V} &\leq \sum_{i=1}^{n}\left(-\frac{e_i^2}{2} + \frac{\xi_i^2}{2}\right) + \frac{\Theta_1(\cdot)}{K} - \frac{\mu_M}{\lambda}\xi^T D^{-1}(q)H(\cdot)\Delta p + \sum_{i=1}^{n} \xi_i^2\{\rho(\cdot) + \hat{\rho}_i(\cdot)\} + \frac{\Theta}{K} \end{aligned} \tag{3.56}$$

where $\Theta = \Theta_1(\cdot) + \Theta_2(\cdot) + \Theta_3(\cdot)$ is an unknown positive constant independent of K.

From Assumption 3.3, we have $\forall h_i(\cdot) > 0$, i.e., the matrix $H(\cdot) = diag\{h_1(\cdot), ..., h_n(\cdot)\}$ is symmetric positive definite. The inverse of inertia matrix $D^{-1}(q)$ is symmetric positive definite. Then the matrix $D^{-1}(q)H(\cdot)$ is also symmetric positive definite. Satisfying

$$\xi^T D^{-1}(q)H(\cdot)\xi \geq 0 \tag{3.57}$$

Select a controller of each coordinate is

$$\Delta p_i = \xi_i \psi_i \tag{3.58}$$

where $\psi_i = 1 + \rho(\cdot) + \hat{\rho}_i(\cdot) > 0$, then the control input vector Δp can be written as

$$\Delta p = \psi \xi \tag{3.59}$$

where the matrix $\psi = diag\{\psi_i, ..., \psi_n\}$ is symmetric positive definite.

Also, observe that

$$\xi^T D^{-1}(q)H(\cdot)\psi\xi \geq 0 \quad \text{or} \quad \xi^T D^{-1}(q)H(\cdot)\Delta p \geq 0 \tag{3.60}$$

together with Property 2.1, it can be shown that

$$\begin{aligned} -\frac{\mu_M}{\lambda}\xi^T D^{-1}(q)H(\cdot)\Delta p &\leq -\frac{1}{\lambda}\xi^T H(\cdot)\Delta p \\ &:= -\sum_{i=1}^{n} \xi_i^2 \frac{h_i(\cdot)}{\lambda}\psi_i \end{aligned} \tag{3.61}$$

From Assumption 3.3, we have

$$\begin{aligned} h(\cdot) &\geq \lambda \\ \frac{h(\cdot)}{\lambda} &\geq 1 \end{aligned} \tag{3.62}$$

Combining (3.61) and (3.62) together, yields

$$\begin{aligned} \dot{V} &\leq -\frac{1}{2}\sum_{i=1}^{n}(e_i^2 + \xi_i^2) + \frac{\Theta}{K} \\ &\leq -bV + \frac{\Theta}{K} \end{aligned} \tag{3.63}$$

where $b = \min\left\{1, \frac{\lambda}{\mu_M}\right\} > 0$.

In the remaining part of the proof, we show that all states $(e, \bar{e}, K)$ of the closed-loop system (3.46), (3.58) and (3.48) are bounded and well-defined on $[0, +\infty)$. Moreover, given any $\varepsilon > 0$ there exists a finite time T_ε such that the position tracking error $\| q - q_r \| \leq \varepsilon$, $\forall t \geq T_\varepsilon$.

Using eq. (3.63), we obtain

$$\dot{V} \leq -bV + \Theta \tag{3.64}$$

which implies that (e, ξ, K) are well-defined on $[0, +\infty)$ and (e, ξ) is bounded. The compact set $\Omega = \left\{e, \xi | V(e, \xi) \leq a, \forall a \geq \frac{\Theta}{b}\right\}$ is invariant, since V is positive definite and proper and $\dot{V}$ is negative semi-definite $\forall e, \xi \in \Omega$. To show that $K(t)$ is bounded, we use a contradiction argument. In particular, suppose that the monotone non-decreasing function $K(t)$ is unbounded. Then there must exist a finite time T^* such that

$$K(t) \geq \frac{\Theta}{\varepsilon^*}, \quad \varepsilon^* = \frac{b\varepsilon^2}{16}, \quad \forall t \geq T^* \tag{3.65}$$

and (3.63) becomes

$$\dot{V} \leq -bV + \varepsilon^*, \quad \forall t \geq T^* \tag{3.66}$$

Consequently,

$$V(t) \leq e^{-b(t-T^*)}(V(T^*) - \frac{\varepsilon^*}{b}) + \frac{\varepsilon^*}{b}, \quad \forall t \geq T^* \tag{3.67}$$

This implies that there exists another finite time T_1 such that

$$\frac{\| q - q_r \|^2}{2} = \frac{1}{2}\sum_{i=1}^{n} \leq V(t) \leq \frac{2\varepsilon^*}{b} = \frac{\varepsilon^*}{8}, \quad \forall t \geq T_1 \tag{3.68}$$

which contradicts the assumption that $K(t)$ is unbounded since $\dot{K}(t) = 0$, $\forall t \geq T_1$.

Since $K(t)$ is bounded, we can conclude that all of the states $(e, \bar{e}, K)$ of equations (3.46), (3.58) and (3.48) are also bounded and well-defined on $[0, +\infty)$. Hence, from Assumption 3.1, the closed-loop system trajectories generated by equations (3.46), (3.58) and (3.48) are well-defined and bounded on $[0, +\infty)$.

In addition, the integral of $\dot{K}(t)$ evaluated from zero to infinity exists and it finite, that is

$$\lim_{t \to +\infty} \int_0^t \dot{K} d\tau = K(\infty) - K(0) \tag{3.69}$$

Then, it follows from *Barbalat 's lemma* that

$$\lim_{t \to +\infty} \dot{K}(t) = 0 \tag{3.70}$$

This, together with equation (3.48), implies the existence of a finite time T_ε satisfying

$$\| q(t) - q_r(t) \| \leq \varepsilon, \quad t \geq T_\varepsilon > 0. \tag{3.71}$$

4 Simulation Example Results

In order to verify the performance of proposed the adaptive control scheme, as an illustration, we will apply the above presented the control scheme to a two-link robot arm actuated by the pneumatic muscles as shown in Fig. 5. The revolute joint 1 is rotatable through an angle $-\pi < q_1 < \pi$ rad. and the revolute joint 2 is rotatable through an angle $-\pi < q_2 < \pi$ rad.

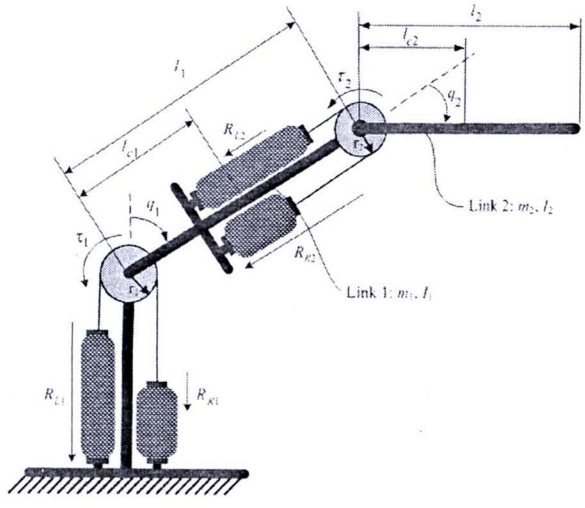

Figure 5: The two-link robot arm actuated by pneumatic muscles.

The dynamic of the two-link robot arm actuated by pneumatic muscles can be described as

$$
\begin{bmatrix} \ddot{q}_1 \\ \ddot{q}_2 \end{bmatrix} = \begin{bmatrix} d_{11} & d_{12} \\ d_{21} & d_{22} \end{bmatrix}^{-1} \left\{ \begin{bmatrix} a_{A1} & 0 \\ 0 & a_{A2} \end{bmatrix} \begin{bmatrix} \Delta p_1^2 \\ \Delta p_2^2 \end{bmatrix} + \begin{bmatrix} h_1(\cdot) & 0 \\ 0 & h_2(\cdot) \end{bmatrix} \begin{bmatrix} \Delta p_1 \\ \Delta p_2 \end{bmatrix} + \begin{bmatrix} b_{E1}(t) & 0 \\ 0 & b_{E2}(t) \end{bmatrix} \begin{bmatrix} \dot{q}_1 \\ \dot{q}_2 \end{bmatrix} + \begin{bmatrix} a_{F1} & 0 \\ 0 & a_{F2} \end{bmatrix} \begin{bmatrix} q_1 \\ q_2 \end{bmatrix} + \begin{bmatrix} a_{G1} \\ a_{G2} \end{bmatrix} - \begin{bmatrix} c_{11} & c_{12} \\ c_{21} & c_{22} \end{bmatrix} \begin{bmatrix} \dot{q}_1 \\ \dot{q}_2 \end{bmatrix} - \begin{bmatrix} f_1 \\ f_2 \end{bmatrix} \right\} \tag{4.72}
$$

where

$$
\begin{aligned}
a_{A1} &= n_1(F_{2L1} + F_{2R1})r_1 \\
a_{A2} &= n_2(F_{2L2} + F_{2R2})r_2 \\
h_1(\cdot) &= b_{B1}(t)\dot{q}_1 + a_{C1}q_1 + a_{D1} \\
h_2(\cdot) &= b_{B2}(t)\dot{q}_2 + a_{C2}q_2 + a_{D2} \\
b_{B1}(t) &= \begin{cases} -n_1(B_{1L1i} + B_{1R1d})r_1^2 & ,\dot{q}_1 < 0 \\ 0 & ,\dot{q}_1 = 0 \\ n_1(B_{1L1d} + B_{1R1i})r_1^2 & ,\dot{q}_1 > 0 \end{cases} \\
b_{B2}(t) &= \begin{cases} -n_2(B_{1L2i} + B_{1R2d})r_2^2 & ,\dot{q}_2 < 0 \\ 0 & ,\dot{q}_2 = 0 \\ n_2(B_{1L2d} + B_{1R2i})r_2^2 & ,\dot{q}_2 < 0 \end{cases} \\
a_{C1} &= n_1(K_{1R1} - K_{1L1})r_1^2 \\
a_{C2} &= n_2(K_{1R2} - K_{1L2})r_2^2 \\
a_{D1} &= n_1(2F_{2R1}P_{0R1} - F_{1R1} + 2F_{2L1}P_{0L1} - F_{1L1} + r_1K_{1R1}\pi + r_1K_{1L1}\pi)r_1 \\
a_{D2} &= n_2(2F_{2R2}P_{0R2} - F_{1R2} + 2F_{2L2}P_{0L2} - F_{1L2} + r_2K_{1R2}\pi + r_2K_{1L2}\pi)r_2 \\
b_{E1}(t) &= \begin{cases} -n_1(B_{0L1i} + B_{1L1i}P_{0L1} + B_{0R1d} - B_{1R1d}P_{0R1})r_1^2 & ,\dot{q}_1 < 0 \\ 0 & ,\dot{q}_1 = 0 \\ -n_1(B_{0L1d} - B_{1L1d}P_{0L1} + B_{0R1i} + B_{1R1i}P_{0R1})r_1^2 & ,\dot{q}_1 > 0 \end{cases} \\
b_{E2}(t) &= \begin{cases} -n_2(B_{0L2i} + B_{1L2i}P_{0L2} + B_{0R2d} - B_{1R2d}P_{0R2})r_2^2 & ,\dot{q}_2 < 0 \\ 0 & ,\dot{q}_2 = 0 \\ -n_2(B_{0L2d} - B_{1L2d}P_{0L2} + B_{0R2i} + B_{1R2i}P_{0R2})r_2^2 & ,\dot{q}_2 > 0 \end{cases} \\
a_{F1} &= -n_1(K_{1L1}P_{0L1} + K_{1R1}P_{0R1} + K_{0L1} + K_{0R1})r_1^2 \\
a_{F2} &= -n_2(K_{1L2}P_{0L2} + K_{1R2}P_{0R2} + K_{0L2} + K_{0R2})r_2^2 \\
a_{G1} &= -n_1(F_{2R1}P_{0R1}^2 - F_{1R1}P_{0R1} - F_{2L1}P_{0L1}^2 + F_{1L1}P_{0L1} \\
&\quad + r_1K_{1R1}P_{0R1}\pi + r_1K_{0R1}\pi - r_1K_{1L1}P_{0L1}\pi - r_1K_{0L1}\pi)r_1 \\
a_{G2} &= -n_2(F_{2R2}P_{0R2}^2 - F_{1R2}P_{0R2} - F_{2L2}P_{0L2}^2 + F_{1L2}P_{0L2} \\
&\quad + r_2K_{1R2}P_{0R2}\pi + r_2K_{0R2}\pi - r_2K_{1L2}P_{0L2}\pi - r_2K_{0L2}\pi)r_2 \\
d_{11} &= m_2(2l_1l_{c2}\cos q_2 + l_{c2}^2 + l_1^2) + m_1l_{c1}^2 + M(2l_1l_2\cos q_2 + l_1^2 + l_2^2) + I_1 + I_2 + I_M \\
d_{12} &= m_2(l_{c2}^2 + l_1l_{c2}\cos q_2) + M(l_2^2 + l_1l_2\cos q_2) + I_2 + I_M \\
d_{21} &= d_{12} \\
d_{22} &= m_2l_{c2}^2 + Ml_2^2 + I_2 + I_M \\
c_{11} &= -(m_2l_1l_{c2} + Ml_1l_2)\dot{q}_2\sin q_2 \\
c_{12} &= -(m_2l_1l_{c2} + Ml_1l_2)(\dot{q}_1 + \dot{q}_2)\sin q_2 \\
c_{21} &= (m_2l_1l_{c2} + Ml_1l_2)\dot{q}_1\sin q_2 \\
c_{22} &= 0 \\
f_1 &= -m_1gl_{c1}\sin q_1 - m_2g(l_1\sin q_1 + l_{c2}\sin(q_1 + q_2)) - Mg(l_1\sin q_1 + l_2\sin(q_1 + q_2)) \\
f_2 &= -(m_2gl_{c2} + Mgl_2)\sin(q_1 + q_2)
\end{aligned}
$$

m_l, m_2, l_1, l_2, l_{c1}, l_{c2}, r_1, r_2, I_1 and I_2 denote the masses and lengths and radius and the inertias of the each link. M and I_M denote the load and the inertia at the end.

We investigate the closed-loop system behaviors of our adaptive control. The two-link planar robot arm studied here is similar to those in Fig. 5. The closed-loop system is simulated with the physical parameters of the arm as follows, $l_1 = 20$ in., $l_{c1} = 10$ in., $l_2 = 20$ in., $l_{c2} = 10$ in., $m_1 = m_2 = 1$ slug, $r_1 = 3$ in. and $r_2 = 2$ in. and the numbers of muscle pairs $n_1 = 6$ and $n_2 = 3$. All of the simulation were performed with the initial conditions, $q_1(0) = q_2(0) = 1$ rad., $\dot{q}_1(0) = \dot{q}_2(0) = 0.01$ rad./s, $\varepsilon = 0.1$ rad., $\beta = 10$ and the nominal pressures, $P_{0R1} = P_{0R2} = 40$ psi. and $P_{0L1} = P_{0L2} = 60$ psi.

In the simulations, we restricted the internal pressure in each muscle within the range, $0 \leq P \leq 130$ psi. since in a real system, the internal pressure can not go below zero and the parameters of the muscles using in here are only valid in this range. In addition, we use the full nonlinear model which includes the terms $a_{Ai}\Delta p_i^2$ when $i = 1, ..., n$.

We studied five cases of the muscle parameter sets as shown in Table 1. The nominal parameters are the ones studied in [4]. The other two sets of coefficients represent 50% increase and 50% decrease of muscle coefficients. Case A represents the system under normal condition and has a matching pair of muscle groups. Case B to Case E represent the cases when the system has a mismatch pair of muscle groups or undergoes severe changes of muscle properties.

Table 1: Case studies for investigate tracking performance.

Case	Bicep1 (b1)	Tricep1 (t1)	Bicep2 (b2)	Tricep2 (t2)
A	Mean	Mean	Mean	Mean
B	+50%	-50%	+50%	-50%
C	-50%	+50%	-50%	+50%
D	+50%	-50%	-50%	+50%
E	-50%	+50%	+50%	-50%

We investigate controller performance by trajectory tracking for the end effector in xy space, i.e., a circle path is given by:

$$x_d = 16 + 8\sin(0.4\pi t) \tag{4.73}$$

$$y_d = 16 + 8\cos(0.4\pi t) \tag{4.74}$$

where x_d and y_d the desired end-effector spatial trajectories along x and y axes. For the inverse kinematics of the planar arm in Fig. 5, it can be to compute that these spatial path requirements are equivalent to required joint trajectories of

$$q_{2r} = \arccos\left(\frac{x_d^2 + y_d^2 - l_1^2 - l_2^2}{2l_1 l_2}\right) \tag{4.75}$$

$$q_{1r} = \arctan\left(\frac{x_d}{y_d}\right) - \arctan\left\{\frac{l_2 \sin q_2}{l_1 + l_2 \cos q_2}\right\} \tag{4.76}$$

Table 2: Load variation at time 0 - 2000 sec.

Time (s)	Load (slug.)
$0 \leq t < 400$	1
$400 \leq t < 800$	0
$800 \leq t < 1200$	1
$1200 \leq t < 1600$	0
$1600 \leq t \leq 2000$	1

We performed the simulations for 2000 sec. under the load variation at the end as follow on Table 2. The simulation results of five cases are shown in Fig. 6-10. The tracking performance in five cases

are shown in Fig. 6. The adaptive gains and tracking errors are shown in Fig. 7 that all cases indicate that the gain defined by (3.48) is monotone nondecreasing and bounded on $[0, +\infty)$. and all cases demonstrated that the tracking error would eventually be within the prescribed error $\varepsilon = 0.1$ rad. after a finite time.

The pressure inputs Δp_1 and Δp_2 are shown in Fig. 8, the internal left muscle pressures of each left muscle P_{L1} and P_{L2} are shown in Fig. 9 and the internal right muscle pressures of each right muscle P_{R1} and P_{R2} are shown in Fig. 10. All cases indicate that internal pressures (P_{L1}, P_{L2}, P_{R1} and P_{R2}) are still within the range $0 \leq P \leq 130$ psi.

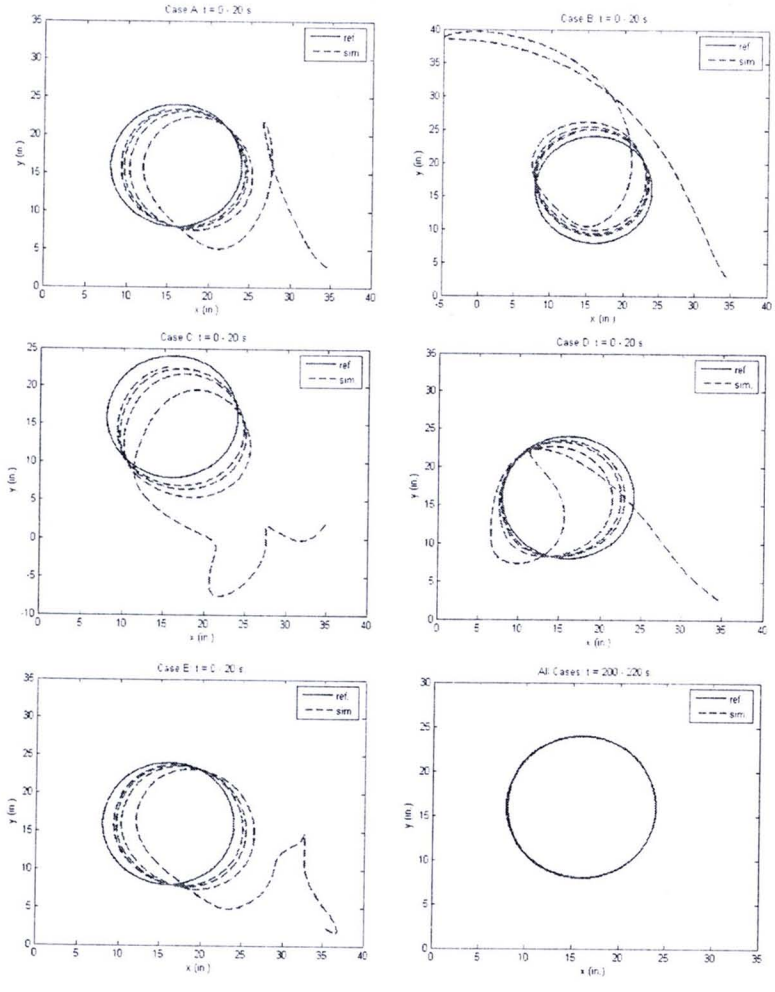

Figure 6: End-effector spatial trajectories

5 Conclusion

We propose an adaptive tracking control scheme for multi-link robots actuated by pneumatic muscles. All of physical parameters of the robot and pneumatic muscles are unknown. Under these conditions, we can proof that the joint angles of the robots can follow any $\mathbf{C}^1$ trajectories. The closed-loop states are globally bounded and the total angle error will be within any nonzero prescribed error in a finite time. We do not assume that the bounds of uncertain time-varying parameters are known a priori. From the simulations, it is shown that our adaptive control scheme can achieve angle tracking even under severe changes of system parameters.

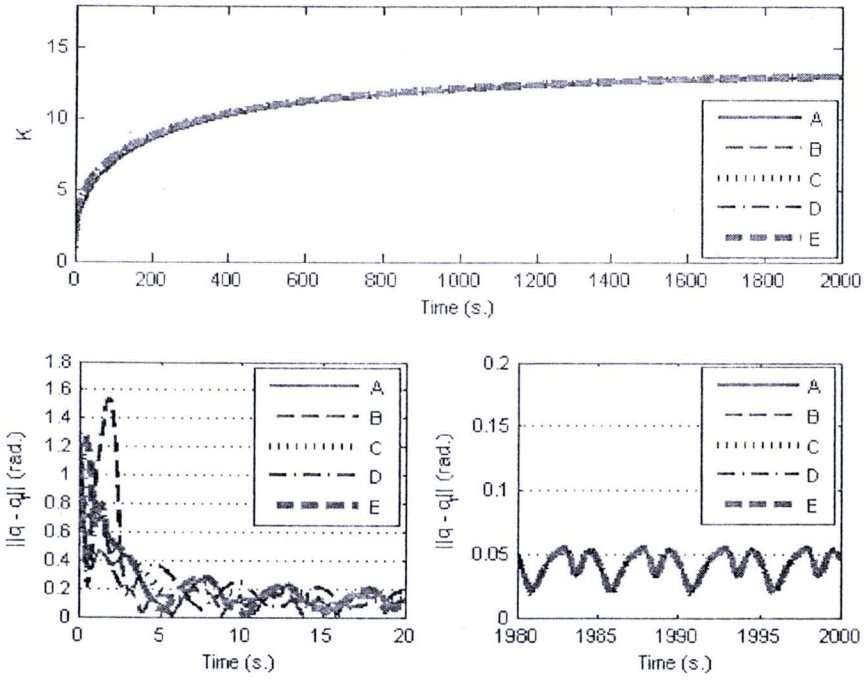

Figure 7: Adaptive gains and the total errors

References

[1] C.P. Chou and B. Hannaford, "Static and Dynamic Characteristics of McKibben Pneumatic Artificial Muscles", *Proc. IEEE International Conference on Robotics and Automation*, San Diego, CA, USA, May 1994.

[2] C. P. Chou and B. Hannaford, "Measurement and Modeling of McKibben Pneumatic Artificial Muscles", *IEEE Trans. on Robotics and Automation*, Vol. 12 (1996), 90-102.

[3] B. Tondu and P. Lopez, "Modeling and Control of McKibben Pneumatic Artificial Muscle Robot Actuators", *IEEE Control Systems Magazine*, vol. 20 (2000), 15-38.

[4] D. B. Reynolds, D. W. Repperger, C. A. Philips and G. Bandry, "Dynamic characteristics of pneumatic muscle", *Computers in Biology and Medicine*, Submitted.

[5] D. B. Reynolds, D. W. Repperger, C. A. Phillips, and G. Bandry, "Modeling the Dynamic characteristics of pneumatic muscle", *Ann. Biomed. Eng.*, vol. 31 (2003), 310-317.

[6] J. Lilly, "Adaptive tracking for pneumatic muscle actuators in bicep and tricep configurations", *IEEE Trans. Neural Systems Rehabilitation Eng.*, vol. 11 (2003), 333-339.

[7] J. Lilly and P. Quesada, "A Two-Input Sliding-Mode Controller for a Planar Arm Actuated by Four Pneumatic Muscle Groups", *IEEE Trans. Neural Syst. Rehabil. Eng.*, vol. 12, (2004), 349-359.

[8] J. Lilly and L. Yang, "Sliding Mode Tracking for Pneumatic Muscle Actuators in Opposing Pair Configuration", *IEEE Trans. Control System Technology*, vol. 13, (2005), 550-558.

[9] X. Chang and J. Lilly, "The Dynamics of PM Arm and Its Control" [online], Available *http://louisville.edu/ x0chan01/res/pms.htm*, 2003.

[10] J. Lilly and X. Chang, "A Fuzzy Model Predictive Controller for a Planar Arm Actuated by Four Pneumatic Muscle Group", ready to submit

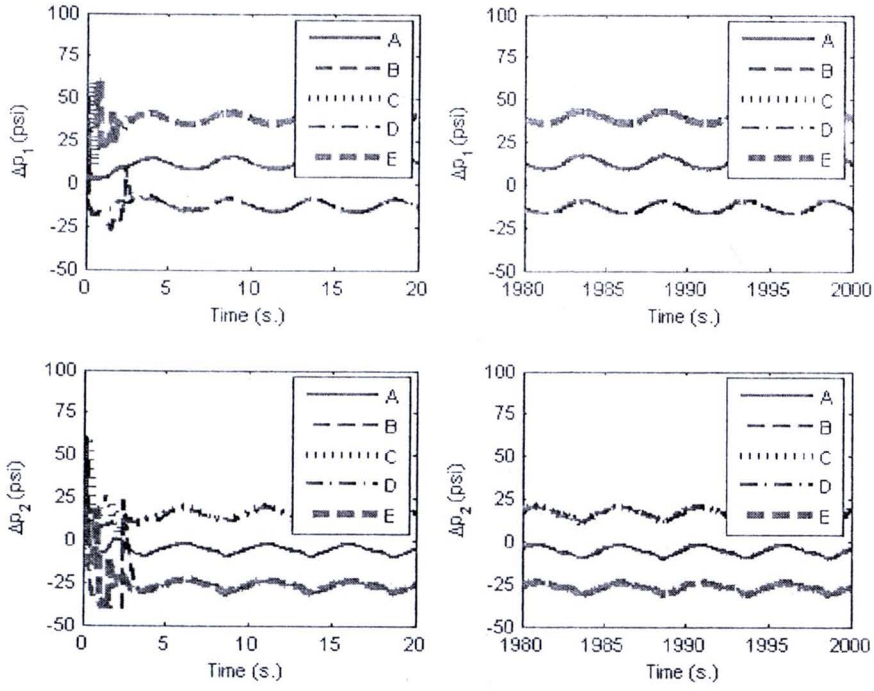

Figure 8: pressure inputs

[11] D.W. Cai and H. Yamaura: "A Robust Controller for Manipulator Driven by Artificial Muscle Actuator", *Proceedings of the IEEE International Conference on Control Applications*, Dearborn, MI, 1996, 540-545.

[12] D.W. Cai and Y. Dai. "A sliding mode controller for manipulator driven by artificial muscle actuator", *Proceedings of IEEE International Conference on Control Applications*, Anchorage, 2000, 668-673.

[13] G. Tonietti and A. Bicchi, "Adaptive simultaneous position and stiffness control for a soft robot arm", *Proceedings of the IEEE/RSJ Conference on Intelligent Robots and Systems EPFL*, Lausanne, Switzerland, vol.2 (2002), 1992-1997.

[14] L. Zhang, J. Xie and D. Lu, "Adaptive Robust Control of One-Link Joint Actuated by Pneumatic Artificial Muscles",*Proceedings of IEEE/ICBBE International Conference on Bioinformatics and Biomedical Engineering*,2007, 1185 - 1189.

[15] X.C. Zhu, G.L. Tao, J. Cao, B. Yao, "Adaptive Robust Posture Control of a Pneumatic Muscles Driven Parallel Manipulator", *4th IFAC Symp. on Mechatronic Systems*, Heidelberg, Germany, 2006, 764-769.

[16] G.L. Tao, X.C. Zhu, B. Yao and J. Cao, "Adaptive Robust Posture Control of a Pneumatic Muscles Driven Parallel Manipulator with Redundancy". *Proceedings of American Control Conference*. New York, USA, 2007, 3408-3413.

[17] W. Lin and R. Pongvuthithum, "Adaptive output tracking of inherently nonlinear systems with nonlinear parameterization", *IEEE Trans. Automatic Control*, vol. 48 (2003), 1737-1349.

[18] R. Pongvuthithum, S. M. Veres, S. B. Gabriel, and E. Rogers, "Universal adaptive control of satellite formation flying", *International Journal of Control*, Vol. 78 (2005), 45-52.

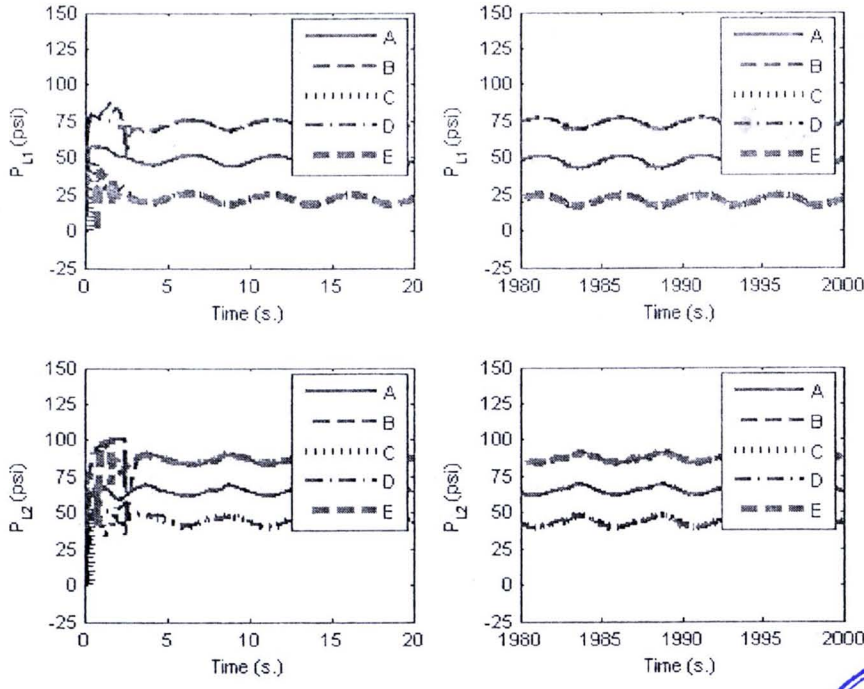

Figure 9: Internal pressures of bicep muscles

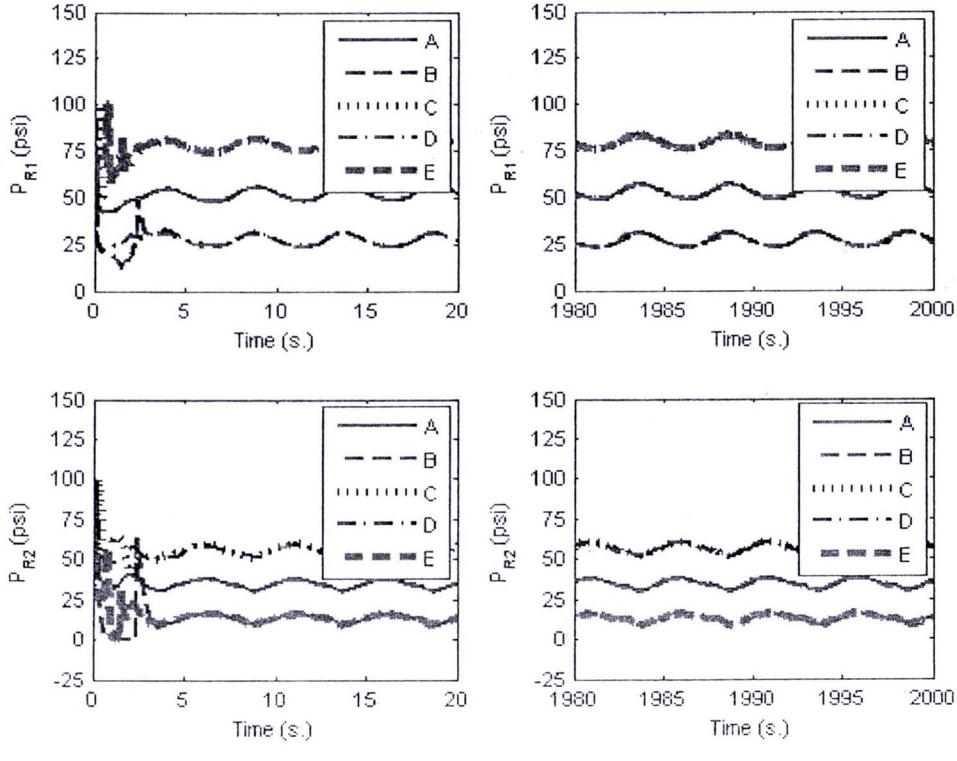

Figure 10: Internal pressures of tricep muscles